The full-scale avalanche test site, Lautaret, France.

Emmanuel THIBERT[1]*, Hervé BELLOT[1], Xavier RAVANAT[1], Frédéric OUSSET[1], Gaëtan PULFER[1], Mohamed NAAIM[1], Florence NAAIM-BOUVET[1], Koichi NISHIMURA[2], Yoichi ITO[2], Djebar BAROUDI[3], Alexander PROKOP[4], Peter SCHÖN[4], P. Alvaro SORUCO[5], Christian VINCENT[6], Ali LIMAM[7], Damianao PESARESI[8].

[1]* IRSTEA, UR ETGR, 2 rue de la Papeterie, 38402 Saint Martin d'Hères Cedex, France.
[2] Nagoya University (Japan)
[3] School of Science and Technology, Aalto University, FIN-00076 Aalto, Finland
[4] Institute of Mountain Risk Engineering, Institute of Mountain Risk Engineering, Vienna, Austria
[5] IGEMA, La Paz, Bolivia
[6] LGGE, CNRS-UJF, Grenoble, France
[7] INSA-Lyon, UR LGCIE, Villeurbanne, France
[8] OGS, Udine (Italy)

ABSTRACT: The Lautaret full-scale avalanche test site in the southern French Alps has been used by IRSTEA (Cemagref) Research Institute since 1973. Over the recent years two avalanche paths are used to release small to medium avalanches 3 or 4 times each winter. Avalanche flows are generally dense, whether wet or dry, sometimes with a powder part. Main path n°2 (track length 800 m) is dedicated to avalanche dynamics. Within the flow of the avalanche, flow height and vertical profiles of pressure and velocity are measured along a 3.5 m tripod. The snow volume released in the starting zone is quantified by a differential analysis of laser scanning measurements set before and after triggering. A high rate positioning of the avalanche along the track is determined from terrestrial oblique photogrammetry. Above the dense layer, the saltation layer and the powder part are characterized by particles and air fluxes measurements. In path n°1 smaller in size, medium-size avalanches (track length 500 m) make this track of particular interest for experiments on structures. A macroscopic sensor-structure is set nearly 150 m downhill from the starting zone, that is, in the area where avalanches generally reach their maximum velocity. It consists is a one square-meter plate supported by a 3.5 m high steel cantilever fixed in the ground, facing the avalanche. Impact pressures are reconstructed from the cantilever deformations, while avalanche velocity is measured from optical sensors. Seismic signals generated by avalanches of those 2 paths are recorded by a 3-axial broadband seismometer. Around those experimental devices dedicated to the understanding of avalanche physics, a national and international partnership has been developed from years to years, including INSA de Lyon, CNRS and Université Joseph Fourier (France), Aalto University (Finland), Nagoya University (Japan), Boku University (Austria), IGEMA (Bolivia), OGS (Italy)

KEYWORDS: Avalanche, test-site, full-scale experiments.

1 SITE

The Lautaret full-scale avalanche test site (southern French Alps, 45.033°N/6.404°E) is owned by the Irstea (previously Cemagref) research institute, and is known to avalanche specialists for its long experimental history, going back to 1973 (Issler, 1999; Barbolini, and Issler, 2006.). Two avalanche paths (Fig. 1) are located on the southeast slope of Mont Chaillol (max. 2600ma.s.l.) near the Lautaret pass (2058 ma.s.l). In path 1, a strong concrete foundation was built specifically to support experiments focusing on avalanche and obstacle interactions, especially impact pressure. In path 2, a 4.0 m high tripod support is located in the track. Small to medium avalanches occur at a sufficient frequency (up to three or four each winter). Avalanche flows are generally dense, wet or dry, with sometimes as mall but fast powder cloud (or saltation layer). The dense part is usually <1 m thick. The avalanche path is 800 m long with an average gradient of 368 in the experimental zone. Typical release volumes vary from 500 to 10 000 m^3, and maximum front speed can reach 30–40 m/s (Meunier and others, 2004). The track length is 500 to 800 m for path 1 and 2, respectively, with an average slope angle of 36° that reaches 40° in the starting zone. Dry snow avalanches released in early winter generally exhibit a density of 80 to 160 kg/m^3 in the starting zone and between 300 and 350 kg/m^3 in the deposition area. Snow deposition by avalanches tures described below are easily cleared of

Corresponding author address: Emmanuel THIBERT, IRSTEA, UR ETGR, Saint Martin d'Hères, France
tel:+33(0)476762813; Fax:+33(0)476513803
email: emmanuel.thibert@irstea.fr

snow and are rapidly operational for the next avalanche release. These conditions make this site of particular interest for experiments involving avalanche impacts on structures. On the North-East slope, a third path has been released a few times in vue to a future instrumentation.

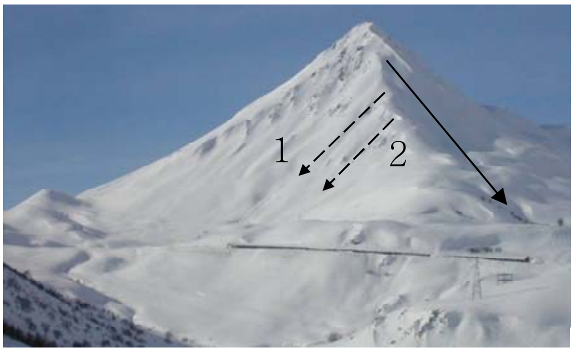

Figure 1. Lautaret avalanche test site on the South-East of the Chaillol Montain where avalanche paths 1 and 2 are regularly triggered. The right arrow is the North-East path not instrument at present.

2 GENERAL EQUIPMENT AND INSTRUMENTATION

2.1 Shelter

A reinforced-concrete shelter for operators and data acquisition is located between two of the main avalanche paths (1 and 2; see Fig. 2), which are separated by around 20 m. The shelter houses the data acquisition equipment including a National Instrument SCXI-1000 and PXI high frequency loggers. A sampling rate of 3 kHz is used to ensure the recording of dynamic effects (pressure, deformation, accelerations measurements by sensors). Dedicated acquisition cards are used for velocity measurements with acquisition rate up to 180 kHz.

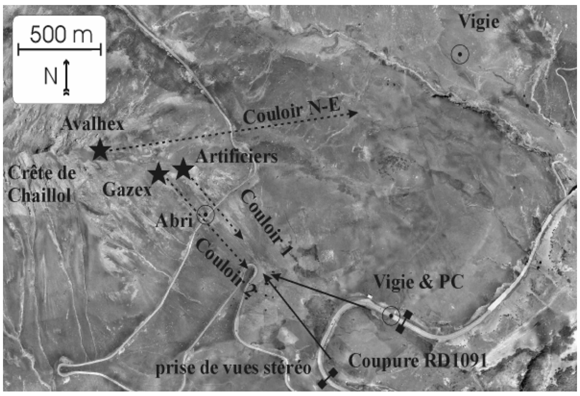

Figure 2. Aerial ortho-photo map of Lautaret site indicating locations of the main equipments.

2.2 Release systems and snow characterisation

Path n°1 is currently released by 2 operators with manual explosive with electric starting. Path n°2 is released with a Gazex radio remote system. This employs a gas explosive tube using a mixture of propane and industrial oxygen (Fig. 3). Information on the snow conditions is obtained performing manual snow-pits close to the release zone. This includes snow density, temperature, hardness as well as grain types and characteristic size. Atmospheric conditions prior to avalanche triggering are monitored by a weather station which records half-hourly averages of air temperature and specific humidity during winter.

Figure 3. The release remote system GazEx used in avalanche path n°2.

2.3 Seismometer

In seismic science, it is sometimes important to decipher an avalanche signal within the natural earth seismic activity and from anthropogenic low frequency (infra-sound) sources. For risk mitigation, estimating remotely the avalanche activity from seismic signals is also an alternative to direct observations which are often limited by the visual conditions and observer's availability. In order to characterize an avalanche signal, a partnership was developed with OGS (Italy). A Guralp CMG40T 3-axis broadband seismometer is used. This seismometer has a flat response curve between 30s and 100 Hz. Data are stored in a Lennartz M24 seismic data-logger whose full scale sensitivity is set at

2.5 V. The sensor is orientated normally with its north-south component towards the geographic north. Its East-West component is then almost aligned with the avalanche path direction (Fig.4).

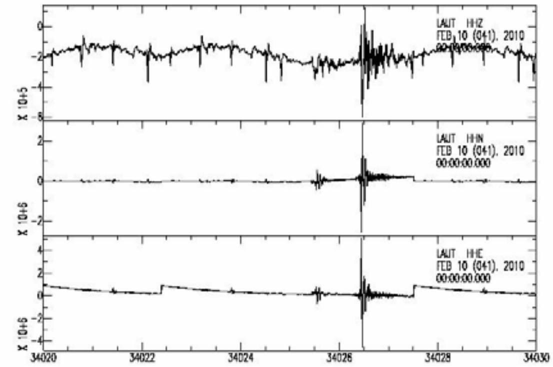

Figure 4. Example of seismic recoding associated to an avalanche release (Pesaresi et al., 2010). Top is Z component, middle is North, bottom is South.

Figure 4 shows seismic recording of the avalanche released of the 10th February 2010. The large variations observed by on the vertical direction (upper panel) is related the thermal effect in the shelter due to the operators in the shelter (air density changes from external atmospheric air entering the shelter; from Pesaresi et al., 2010).

3 AVALANCHE DYNAMICS DEDICATED INSTRUMENTATION

3.1 Pressure and velocity measurements

Avalanche dynamic is specifically studied in the largest avalanche path n°2. A 3.5 m in height tripod made of steel is set up in this path at the end of its steepest part (around 2100 m), i.e. where avalanches are expected to reach their maximal velocity (Figure 5). At this location velocity is measured help of optical sensors as developed initially by Dent et al. (1998) and applied at Vallée de LaSionne (VDLS) avalanche test site (Kern et al., 2009, 2010). They exploit the correlation of time-lagged optical signals.

Velocity measurements are a typical example of sensors specifically developed for avalanche science as no equivalent is available commercially. Optical velocity sensors are placed vertically into the flow each 12,5 cm of the side of the tripod. Sensors are mounted in steel wedges to ensure proper contact with the flow. Same sensors are used in path n°1 (see section 4). The mean flow deflection is about of 15° up or down (Figure 5). The principle of optical velocity measurement requires that grains and snow particles aggregates within the flow does not change significantly in relative position during the travel over a short distance d so that their optical backscattering remains self-correlated with a time lag τ. From this, the velocity u of the passing flow can be estimated as $v = d/\tau$. Our optical velocity sensors have been first improved and adapted to laboratory-scale and snow-chute (Bouchet et al., 2003; Rognon et al., 2008). At Lautaret full-scale avalanche test site, we set d =0.00762 m, one fourth of the flow-wise spacing used at VDLS where larger velocities are observed.

Figure 5. Tripod set in avalanche path n°2 holding velocity sensors, pressure sensors and height sensors.

The impact pressure of the flow is also measured vertically on the tripod each 25 cm with classical load cells from FGP. These have just been slightly modified from the commercial units to ensure a strong protection of the wires. They are set up on the hill-face of the tripod (Fig. 6). Height sensors are set up the side of the tripod: they consist in stainless steel plates whose deformations are measured with strain gages. Deformation signal are converted in pressure values used to detect if the load is due to the dense part of the flow. Sensors are equivalent in principle as pressure sensors used at Vallée de La Sionne (Baroudi et al., 2011).

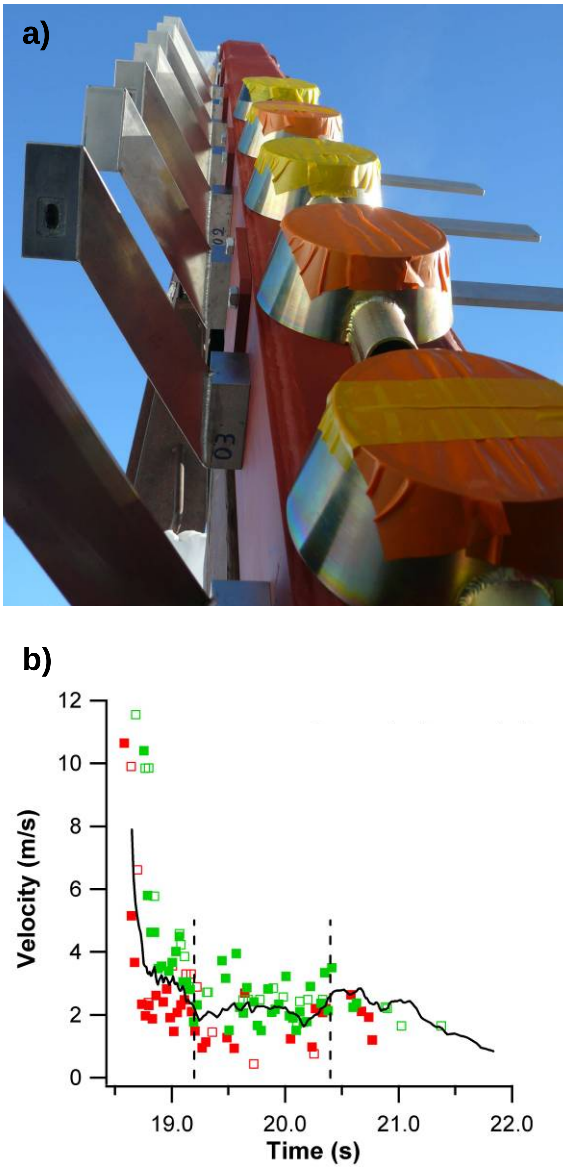

Figure 6. a) Optical velocity sensors imbedded in stainless steel wedges to insure a proper contact with the flow and pressure sensors. b) An example of velocity time plot (data plot from sensors in path n°1)

Figure 7 is an illustration of combining pressure and velocity measurements to analyse the impact pressure developed by an avalanche on a given structure. This one depends on the free pressure of the incident flow (equal to the kinetic energy per unit mass = product of density times the square of the velocity) and on the drag coefficient. Measuring impact pressure and flow velocity simultaneously can therefore give an experimental measurement of the drag coefficient which is not accessible without knowledge of the constitutive law of snow.

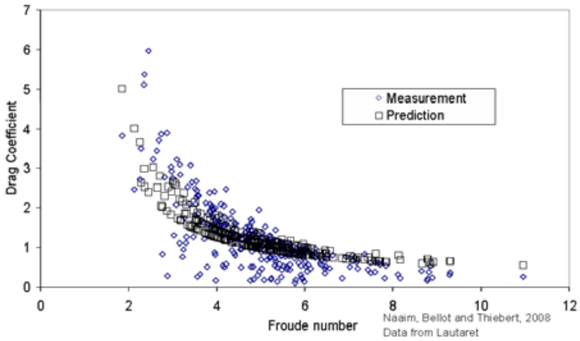

Figure 7. Drag coefficient retrieved from the simultaneous measurement of impact pressure and velocity. Results are compared with prediction from a theoretical framework developed in Naaim et al., 2008.

3.2 Measurement of Voellmy friction parameters

Avalanche fronts in path n°2 are tracked thanks to a high rate photogrammetric system that we have developed with IGEMA (Bolivia) and CNRS (LGGE research unit). Positioning avalanche in time, a velocity of the front is calculated from which Voellmy friction parameters can be retrieved (Soruco et al., 2011)

Terrestrial photogrammetry is the only method able to instantaneously produce digital elevation model during an avalanche flow. Recent advances on digital commercial cameras allow acquiring up to 4 - 8 frames per second with high resolution quality. Cameras are numerical reflex Nikon D2Xs with a Nikon 85mm f/1.4 AF fix focal lens. The overall avalanche path n°2 can be measured with one stereoscopic pair. As a non metric system is used, a calibration is required: the distortions of the lens, the principal point and the focal length have to be measured. We found a slight negative pincushion distortion reaching 10 µm at corners which is typical for long focal length lenses. The focal length is 80.51 mm, and the radial decentration is 80 microns. Calibration is therefore unavoidable.

The Photogrammetric method follows 2 mains steps: image orientation and the photogrammetric restitution (stereo plotting). We use 16 GCPs for the triangulation step. The orientation residual on ground control points in XYZ is around 10 cm, so that a positioning error for restituted points is expected to be les than 25 cm. The last step of the photogrammetric method is the measurement of three-dimensional coordinates on the photographs. In our case, we perform a manual stereo plotting in order to increase the accuracy, and due to the different pixels scale over each photographs which tends to corrupt stereo-correlation. Figure 8 is an illustration of the successive positions of the avalanche released on the 19th December 2012 as tracked by photogrammetry. Basal friction parameters can be retrieved for example by the simple slide block model or more complex shallow water approximation-based models with a Voellmy or a granular material formulation of the friction law (Pulfer et al., 2013).

3.2 Saltation layer and powder part characterization

New devices have been set up over the last 2 years to investigate the internal structure of powder part of avalanches released in path n°2. This research is developed with a specific collaboration with Nagoya University (Japan). An ultrasonic anemometer and a snow particle counter (SPC) have been set on top of the tripod (Figure 9). The ultrasonic anemometer shows the three-dimensional wind direction and speed in the powder cloud. The SPC output usually shows the number of particles and particle diameter at each second for mass flux calculation in the blowing snow. However, the diameter and velocity of the snow particles can also be calculated from the high-frequency recorded data of SPC raw signals. These outcomes reveal the evolution of the powder cloud since the wind speed and particle diameter play a crucial role in the powder cloud development. The first results are presented in this issue by Ito et al. (2013).

Figure 9. Snow particle counter (on left) and ultrasonic anemometer (at center) set up on top of the tripod in path n°2.

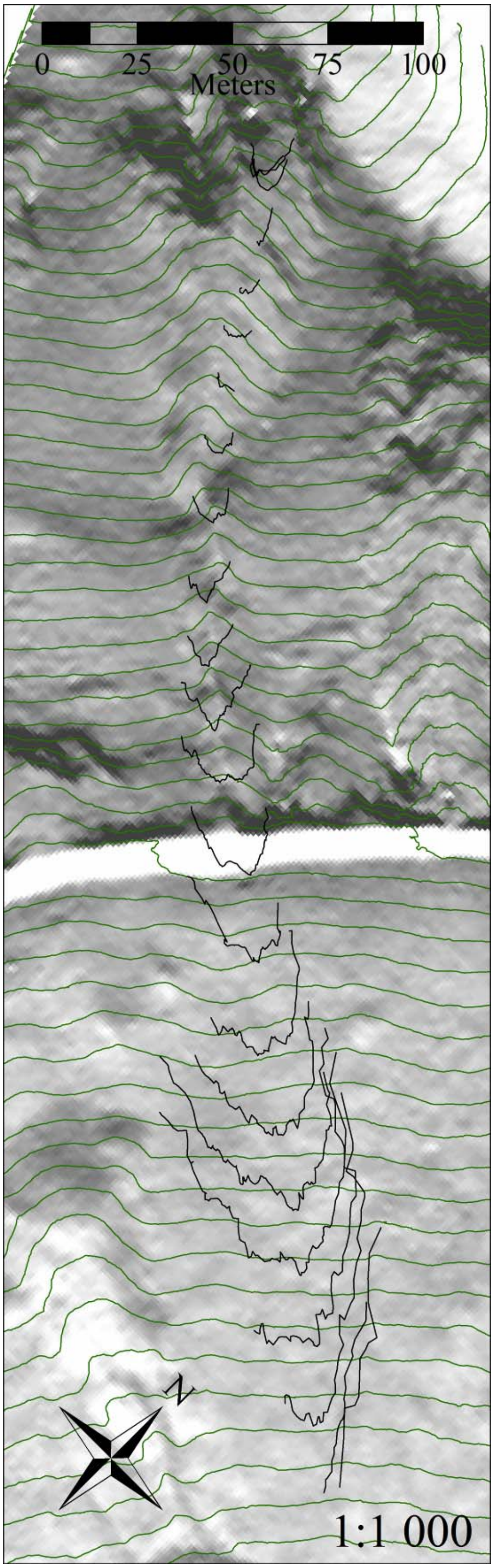

Figure 8. Successive avalanche front positions as tracked from our photogrammetric system on the 19th December 2012 (Pulfer et al., 2013).

3.3 Initial volume released and mass balance

This volume is obtained from digital elevation models of the snow surface from terrestrial laser scanning. We have developed a specific collaboration with BOKU (Austria) for this purpose. The laser we used is the Riegl-321 terrestrial laser scanner operating in a wavelength of 900 nm, which is suitable for snow surfaces (Prokop, 2008). In order to detect changes in the snow surface resulting from the avalanche, we had to take two successive scans of the avalanche path, prior and after the avalanche. Data post processing (registration, filtering, and change detection) was done using the method of Prokop and Panholzer 2009. A detailed description of a laser scanning survey is given in this volume by Prokop et al. 2013. Figure 10 shows elevation changes obtained from digital elevation model difference, indicating volume transfer due to the avalanche (13 February 2013).

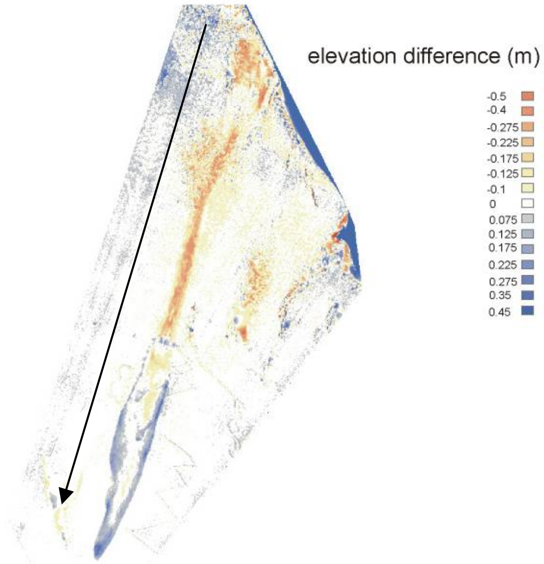

Figure 10. Example of elevation difference measured by laser scan for the avalanche released in path n°2 on the 13 February 2013. The avalanche track (black arrow) is nearly 370 m.

4. IMPACT PRESSURE AND FLOW-OBSTACLE INTERACTIONS

Path n°1, smaller in size than path n°2, and where medium-size avalanches generally develop makes this track of particular interest for experiments on structures, impact pressure and interaction with the flow (snow deposits, etc...). This research has been developed for nearly ten years with INSA-Lyon (LGCIE research unit) and Aalto University in Finland (structural mechanics department), see e.g. Berthet-Rambaud and co-authors (2008) as well as Thibert et Baroudi (2010).

4.1 The structure and its deformation

The instrumented structure is a one square-meter plate supported by a 3.5 m high steel cantilever, facing the avalanche, and fixed in a strong concrete foundation (Fig. 11). The plate can be moved along the beam to be located exactly at the surface of the initial snow-cover prior to avalanche release. It represents a large obstacle in comparison to the flow height and therefore integrates the effects of flow heterogeneities. Strains are measured at the bottom of the beam with precision strain gages placed in the maximum bending moment area. Sampling rate for data acquisition is set at 3000 Hz to record dynamic effects. Signals are filtered with a cut-off frequency of 1000 Hz to ensure a bandwidth without aliasing.

Figure 11. The instrumented structure set up in path n° 1: the beam and the 1 m^2 plate system whose loading is used to reconstruct impact pressure from avalanches. The insight is a velocity sensor set up on the hillside of the plate.

4.2 Pressure reconstruction

The inverse analysis procedure is developed using dynamic strain measurements performed at the bottom of the structure. The avalanche action is assumed to be uniformly distributed over the plate. No avalanche force is assumed to act directly on the beam which is designed to remain elastic during avalanche loading, perfectly clamped at one end and free elsewhere.

The equations of motion are those of structural dynamics (Gerardin and Rixen, 1993) and an Euler-Bernoulli beam model is used.

The direct problem consists in evaluating the strain history from the loading, boundary and initial conditions. Using the Euler-Bernoulli beam model, the direct problem is firstly solved by assuming that the impacting force acts at a specific point. As described by Meirovitch (1986), this formulation is equivalent to solving a Fredholm integral equation of the first order:

$$\varepsilon_i(t) = \sum_j \int_0^t h_{ij}(t-\tau) f_j(\tau) d\tau \tag{1}$$

where ε_i is the strain history measured at a point x_i (gage locations), f_j the impact load at x_j (center of the plate) and h_{ij} the transfer function between excitation and measurement points. The transfer function or its equivalent Frequency Response Function (FRF) in the frequency domain (ω: angular frequency), $\hat{h}(\omega)$, is known once the mechanical model of the structure including its boundary conditions has been set (Fig. 12). The FRFs can be also directly measured from impact hammer tests or calculated from numerical finite element computations (Thibert et al., 2008). As explained in that paper, we use the analytical Euler-Bernoulli beam model in good agreement with the 2 other possible calculations of the FRF.

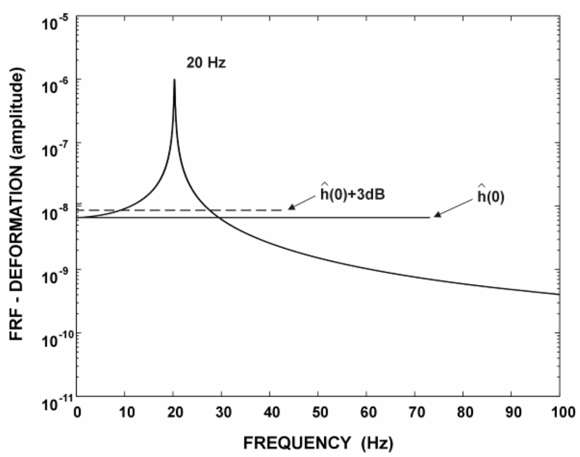

Figure 12: FRF as deduced from the Euler-Bernoulli direct model. Note that the value of 18.6 Hz was measured during hammer tests.

The reconstructed avalanche load is obtained from the solution of the inverse problem given by the regularized deconvolution formula:

$$\hat{f}_\delta(\omega) = \frac{\hat{\varepsilon}^\delta(\omega) \cdot \hat{\phi}(\omega)}{\hat{h}(\omega)}, \tag{2}$$

where the symbol " ^ "denotes Fourier transform functions of the angular frequency variable ω, and Φ is the regularization low pass filter. Given that the FRF can have very small amplitudes and that the measured signal, $\varepsilon_i(t)$, is polluted by noise, the direct deconvolution of Eq. (2) without regularization (Φ =1) can lead to an instability of the inverse problem (Tikhonov and Arsenin, 1977). The answer is therefore to determine the optimal level of regularization, striking a balance between stability and accuracy. This optimal level is achieved using the Morozov discrepancy principle as explained in our previous studies (Baroudi and Thibert, 2009). From that paper, it was estimated that pressure is reconstructed within a relative error of 10%. Figure 13 plots a reconstructed pressure signal (avalanche 15 February 2007).

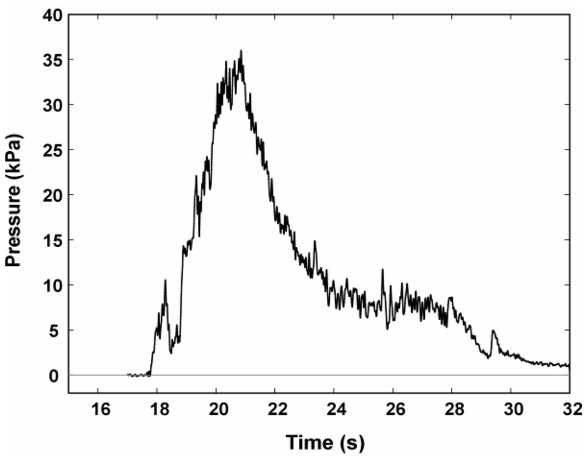

Figure 13: Reconstructed pressure for the avalanche released on 15 February 2007 (Thibert et al., 2008).

Velocity measurements are also performed in path n°1 using the same measurement principle as sensors set up on the tripod in path n°2. Optical velocity sensors are placed 0.35 and 0.65 m vertically above the bottom of the plate and flush laterally on the hillsides. Sensors are mounted in steel wedges to ensure proper contact with the flow. The mean flow deflection is about of 15° relative to a normal impact of the plate. Figure 6 is the plot of the velocity signals obtained for an avalanche released on the 18 March 2011.

These pressure signals coupled with the velocity measurements provide essential full-scale data to estimate the impact pressure of an avalanche on an obstacle. This depends on the free pressure of the avalanche flow and the obstacle drag coefficient. It is a function of the velocity of the avalanches but presents a complex dependence according to the relative contribution of the inertial and gravitational flow regimes (Sovilla et al., 2007, 2008, 2010; Gauer et al., 2007, Baroudi and Thibert, 2009). Recent advances about that specific topic are presented in the present issue (Thibert et al., 2013).

5 REFERENCES

The authors are grateful to all those who contribute to avalanche release operations. Since 2005, experiments and instrumentation have been funded by ANR, INTERREG-Alcotra, PARN.

6 REFERENCES

Barbolini, M. and Issler, D. (Eds.):, 2006. Avalanche test sites and research equipment in Europe: an updated overview. Final Report Deliverable D8, SATSIE Avalanche Studies and Model Validation in Europe, 172 pp.

Baroudi D., and Thibert, E, 2009. An instrumented structure to measure avalanche impact pressure: error analysis from Monte Carlo Simulations. Cold Reg. Sci. Tech., 59(2-3), 242-250.

Baroudi D., B. Sovilla and E. Thibert, 2011. Effect of flow regime and sensor geometry on snow avalanche impact pressure measurements. J. of Glaciology, 57(202), 277-288.

Berthet-Rambaud P., Baroudi D., A. Limam, E. Thibert, Taillandier J.-M., 2008. Characterization of avalanche loading on impacted structures: a new approach based on inverses analysis. Journal of Glaciology, 54(185), 324-332.

Bouchet A., Naaim, M., Ousset, F., Bellot, H., Cauvard, D., 2003. Experimental determination of constitutive equations for dense and dry avalanches: presentation of the set-up and first results. Surveys in Geophysics 24: 525 – 541.

Dent, J.D., Burrell, K.J., Schmidt, D.S., Louge, M.Y., Adams, E. and Jazbutis, T.G., 1998. Density, velocity and friction measurements in a dry snow avalanche. Ann. Glaciol., 26, 247-252.

Gauer, P., Issler, D., Lied, K., Kristensen, K., Iwe, H., Lied, E., Rammer, L., Schreiber, H., 2007. On full-scale avalanche measurements at the Ryggfonn test site, Norway. Cold Reg. Sci. Tech., 49, 39-53.

Gerardin, M. and Rixen, D., 1993. Théorie des vibrations: application à la dynamique des structures. Masson, Paris.

Issler, D., 1999. European Avalanche test sites. Overview and analysis in view of coordinated experiments. Issler, D. (Ed.), Eidg. Inst. Schnee und Lawinenforsch, Mitt. 59.

Kern, M., P. Bartelt, B. Sovilla and O. Buser. 2009. Measured shear rates in large dry and wet snow avalanches. J. Glaciol., 55(190), 327–338.

Kern, M.A., P. Bartelt, B. Sovilla, 2010. Velocity profile inversion in dense avalanche flow. Ann. Glaciol., 51(54), 27-31.

Meirovitch, L., 1986. Elements of vibration analysis. McGraw-Hill, New York, 2nd edition.

Naaim M., T. Faug, E. Thibert, N. Eckert, G. Chambon, F. Naaim and H. Bellot, 2008. Snow avalanches pressure on obstacles. Proceedings of the International Snow Science Workshop 2008, 21-27 September 2008, Whistler, BC, Canada, International Snow Science Workshop Canada Inc. (eds), pp. 740-746.

Prokop, A., 2008. Assessing the applicability of terrestrial laser scanning for spatial snow depth measurements, Cold Regions Sci. Tech., 54, pp. 155–163.

Prokop, A. and Panholzer, H., 2009. Assessing the capability of terrestrial laser scanning for monitoring slow moving landslides, Nat. Hazards Earth Syst. Sci., 9, pp. 1921–1928.

Prokop, A., Schön, P., Singer, F., Pulfer, G., Naaim, M., Thibert E., Determining Avalanche Modelling Input Parameters using Terrestrial Laser Scanning Technology. Procceeding of the International Snow Science Workshop 2013, Grenoble-Chamonix, 6-11 October 2013 (This issue).

Pulfer, G., M. Naaim, E. Thibert and A. Soruco, 2013. Retrieving avalanche basal friction law parameters from high rate positioning of avalanches. Procceeding of the International Snow Science Workshop 2013, Grenoble-Chamonix, 6-11 October 2013 (This issue).

Rognon, P.G., Chevoir, F., Bellot, H., Ousset, F., Naaim, M., Coussot, P., 2008. Rheology of dense snow flows: Inferences from steady state chute-flow experiments. J. Rheol. 52(3), 729-748.

Sovilla, B., Shaer, M., Rammer, L., 2007. Measurements and analysis of full-scale avalanche impact pressure at Vallée de la Sionne test site. Cold Reg. Sci. Tech., doi: 10.1016/j.colregions.2007.05.006.

Sovilla, B., Schaer, M., Kern, M., Bartelt, P., 2008. Impact pressures and flow regimes in dense snow avalanches observed at the Vallée de la Sionne test site. Journal of Geophysical Research 113(1), F01010.

Sovilla, B., McElwaine, J.N., Schaer, M., Vallet, J., 2010. Variation of deposition depth with slope angle in snow avalanches: Measurements from Vallée de la Sionne, J. Geophys. Res., 115, F02016.

Soruco, A., E. Thibert, C. Vincent, R. Blanc, and R. Héno., 2011. Measurement of avalanche front velocity from high-speed terrestrial digital photogrammetry, Geophysical Research Abstracts Vol. 13, EGU2011-8177, 2011.

Tikhonov, A.N. and Arsenin, V.Y, 1977. Solutions of ill-posed problems. Wiley, Chichester (England).

Thibert, E., D. Baroudi, A. Limam, P. Berthet-Rambaud., 2008. Avalanche impact pressure on an instrumented structure. Cold Reg. Sci. Tech., 54, 206-215.

Thibert E. and D. Baroudi, 2010. Impact energy of an avalanche on a structure. Ann. Glaciol., 51(54), 19-28.

Thibert E., T. Faug, H. Bellot and D. Baroudi, 2013. Avalanche impact pressure on a plate-like obstacle. Procceding of the International Snow Science Workshop 2013, Grenoble-Chamonix, 6-11 October 2013 (This issue).